Heliyon 10 (2024) e23077

Contents lists available at ScienceDirect

Heliyon

journal homepage: www.cell.com/heliyon

Hirudin inhibit the formation of NLRP3 inflammasome in cardiomyocytes via suppressing oxidative stress and activating mitophagy

Gang Luo [a,1], Li Chen [a,1], Mingtai Chen [b,c,1], Linshen Mao [a,1], Qihu Zeng [a], Yuan Zou [d], Jinyi Xue [d], Ping Liu [a], Qibiao Wu [b,**], Sijin Yang [a,b,***], Mengnan Liu [a,b,*]

[a] National Traditional Chinese Medicine Clinical Research Base and Department of Cardiovascular Medicine, the Affiliated Traditional Chinese Medicine Hospital, Southwest Medical University, Luzhou, Sichuan, PR China
[b] Faculty of Chinese Medicine and State Key Laboratory of Quality Research in Chinese Medicine, Macau University of Science and Technology, Tapai, Macau
[c] Department of Cardiovascular Disease, Shenzhen Traditional Chinese Medicine Hospital, Shenzhen, Guangdong, China
[d] School of Integrated Traditional and Western Medicine, Southwest Medical University, Luzhou, Sichuan, China

ARTICLE INFO

Keywords:
AngII
Cardiac hypertrophy
H9C2 cells
Hirudin
Mitophagy
NLRP3 inflammasome

ABSTRACT

Context: Cardiomyocyte hypertrophy due to hemodynamic overload eventually leads to heart failure. Hirudin has been widely used in the treatment of cardiovascular diseases and NLRP3 inflammasome was proven to induce cardiomyocyte pyroptosis. However, the mechanism by which it inhibits cardiomyocyte hypertrophy remains unclear.
Objective: To explore the mechanism of hirudin inhibiting cardiomyocyte hypertrophy based on NLRP3 inflammasome activation and mitophagy.
Materials & methods: 1 μM AngII was used for cardiac hypertrophy modeling in H9C2 cells, and cell viability was quantified by CCK-8 assay to screen the appropriate action concentrations of hirudin. After that, we cultured AngII induced-H9C2 cells for 24 h with 0, 0.3, 0.6, and 1.2 mM hirudin, respectively. Next, we marked H9C2 cells with phalloidine and observed them using fluorescence microscope. IL-1β, IL-18, IL-6, TNF-α, ANP, BNP, β-MHC, and mtDNA were analyzed by qRT-PCR; ROS were quantified by Flow cytometry; SOD, MDA, and GSH-Px were detected by ELISA; and proteins including NLRP3, ASC, caspase-1, pro-caspase-1, IL-1β, IL-18, PINK-1, Parkin, beclin-1, LC3-I, LC3-II, p62, were quantified by western blotting.
Results: It was discovered that hirudin reduced the superficial area of AngII-induced H9C2 cells and inhibited the AngII-induced up-regulation of ANP, BNP, and β-MHC. Besides, hirudin down-regulated the expressions of NLRP3 inflammasome-related cytokines, containing IL-1β, IL-18, IL-6, TNF-α. It also down-regulated the expression of mtDNA and ROS, decreased the expression levels of NLRP3 inflammasome activation related proteins, including NLRP3, ASC, caspase-1, pro-

* Corresponding author. National Traditional Chinese Medicine Clinical Research Base and Department of Cardiovascular Medicine, the Affiliated Traditional Chinese Medicine Hospital, Southwest Medical University, Luzhou, Sichuan, PR China.
** Corresponding author.
*** Corresponding author. National Traditional Chinese Medicine Clinical Research Base, the Affiliated Traditional Chinese Medicine Hospital of Southwest Medical University, Luzhou, Sichuan, China.
E-mail addresses: qbwu@must.edu.mo (Q. Wu), ysjimn@sina.com (S. Yang), liumengnan@swmu.edu.cn (M. Liu).
[1] Equal contributors and co-first authors.

https://doi.org/10.1016/j.heliyon.2023.e23077
Received 23 May 2023; Received in revised form 26 November 2023; Accepted 27 November 2023
Available online 2 December 2023

caspase-1, IL-1β, IL-18; and increased the expressions of PINK-1, Parkin, beclin-1, LC3-II/LC3-I, p62 in AngII-induced H9C2 cells.
Discussion: Hirudin promoted the process of mitophagy, inhibited the development of inflammation and oxidative stress, and inhibited the activation of the NLRP3 inflammasome and the PINK-1/Parkin pathway.
Conclusion: Hirudin has the activity to suppress cardiac hypertrophy may benefit from the inhibition of NLRP3 inflammasome and activating of PINK-1/Parkin related-mitophagy.

1. Introduction

When the heart endures overload or injury, the heart muscle develops a compensatory mechanism called myocardial hypertrophy, which can further progress into heart failure [1]. Myocardial hypertrophy usually occurs in conditions such as hypertension, left ventricular outflow tract obstruction, and cor pulmonale. As studies have shown, oxidative stress and inflammation are key factors in the formation of myocardial hypertrophy. Serious studies have reported that inhibiting the activation of oxidative stress and inflammation could prevent myocardial hypertrophy [2,3]. NLRP3 inflammasome belongs to the NOD-like receptor family, which is activated by the assembly of NOD-like receptor pyrin domain containing 3 (NLRP3), apoptosis-related specular protein (ASC), and Pro-Caspase-1 [4–6]. The NLRP3 inflammasome promotes myocardial hypertrophy by activating Caspase-1 and releasing interleukin-1β (IL-1β) and IL-18.

In recent years, studies have investigated the molecular mechanism of NLRP3 activation, which is related to the generation of mitochondrial reactive oxygen species (ROS) [7,8]. Angiotensin II is a known inducer of myocardial hypertrophy in scientific research; it also increases cardiac mitochondrial ROS production [9]. Additionally, mitochondria are abundant in cardiac muscle cells, and mitophagy reflects the autophagy of myocardial apoptosis. However, the autophagy of myocardial hypertrophy has dual effects. On one hand, autophagy could alleviate myocardial hypertrophy and enhance the contractility of the cardiac. On the other hand, if autophagy was continually and excessively activated, it can transform compensatory cardiac hypertrophy into pump failure [10].

Hirudin, an acidic polypeptide composed of 64–66 amino acids isolated from the salivary gland secretions of the leech, is an effective thrombin-specific inhibitor [11]. In traditional Chinese medicine, leeches are used to promote blood circulation, alleviate stasis, and improve collateral vessel flow. With the advancement of medicine, hirudin has gradually been recognized for its additional medicinal values, such as reducing the risk of bleeding and enhancing the efficacy of antithrombotic [12]. Our recent study demonstrated that hirudin possesses inhibitory activity against myocardial hypertrophy. We found that hirudin exerts its effects by regulating PI3K/AKT signaling pathway [13]. In this study, through a series of experiments, we investigated the impact of hirudin on myocardial hypertrophy. This study focuses on the interrelationship between NLRP3 inflammasome and mitophagy as an entry point to illustrate the mechanism of action of hirudin.

2. Materials and methods

2.1. Cell culture and treatment

H9C2 cells were obtained from Procell (no. CL-0089, Wuhan, China). Cells were cultured in Dulbecco's Modified Eagle's Medium (DMEM) supplemented with 10 % fetal bovine serum and maintained at 37 °C with a 5 % CO_2 atmosphere. Cultured H9C2 cells were pretreated for 12 h, 24 h, or 36 h, respectively with 0.01, 0.1, 1, or 10 μM AngII (no. A9525, Sigma-Aldrich, Japan), to screen an optimal concentration and time of AngII. Then H9C2 cells were used to assess if hirudin had a toxic effect on them, cultured H9C2 cells with hirudin (no. H7016, Sigma-Aldrich, Japan) at 0.15, 0.3, 0.6, 1.2 mM concentrations. Finally, 1 μM AngII was used to treat H9C2 cells for 24 h, and 1 μM AngII with 0.3, 0.6, and 1.2 mM hirudin were co-cultured for 24 h, respectively.

2.2. CCK-8 assay

The assay cell counting kit-8 (CCK-8) (no. C0037, Beyotime, China) was utilized to determine the optimal concentration of AngII and hirudin, as well as to assess any potential toxic effects of hirudin on the H9C2 cells. H9C2 cells were cultured to the logarithmic growth phase. 1×10^5/mL cell suspension was prepared with the pre-warmed medium and then seeded into a 96-well cell culture plate after digestion. Once the cells have adhered, the original medium was removed. Cells were treated as described in the cell culture and treatment methods, with PBS serving as a control. On the following day, 10 μl CCK-8 solution was added to per well, and cultured for 4 h, the absorbance of each well was measured at 450 nm using a full spectrum microplate reader (Thermo, USA).

2.3. Rhodamine phalloidin immunofluorescent staining

Cultured H9C2 cells for 24 h with 1 μM AngII and 0, 0.3, 0.6, and 1.2 mM hirudin, respectively, phosphate buffer saline (PBS) as control. Rhodamine phalloidin was used to label β-Actin, a cytoskeletal protein [14]. Remove the medium and fix the cells with 4 % paraformaldehyde. After that, washed it thrice with PBS. Then fixed cells were treated with 0.1 % Triton x-100 for 15 min, and washed thrice. Added rhodamine-phalloidin (no. P2141, sigma-aldrich, Japan) and maintained at 37 °C for 30 min. Finally, added DAPI (no.

D9542, sigma-aldrich, Japan), maintained at room temperature for 10 min. The images were collected by inverted fluorescence microscope (Olympus, Japan) and a microphotography system, and the red area (μm [2]) was calculated by a halo analysis system.

2.4. Transmission electron microscopy (TEM)

The autophagy level of H9C2 cells was observed by TEM as previously research [15]. In brief, cells were prefixed with a 3 % glutaraldehyde after drugs treatment. Followd postfix, dehydrate, infiltrate, and embed. Samples were stained with methylene blue and Ultrathin sections were cut, stained with uranyl acetate and lead citrate. A JEM-1400-FLASH Transmission Electron Microscope (JEOL, Japan) was employed to observe sections.

2.5. Quantitative real-time PCR (qRT-PCR)

Total RNA from samples was extracted by trizol reagent based on the manufacturer's instructions (no. 15596026, Invitrogen, USA). To quantify the expression of IL-1β, IL-18, IL-6, tumor necrosis factor-α (TNF-α), atrial natriuretic peptide (ANP), brain natriuretic peptide (BNP), β-myosin heavy chain (β-MHC) and mitochondrial DNA (mtDNA), samples were conducted by sybr green assay (no. Q221-01, Vazyme, China) based on the manufacturer's protocol. β-actin or GAPDH acted as a control and the $2^{-\Delta\Delta Ct}$ method was used to quantify the expression levels of relative genes. The qPCR conditions as list as follows: 95 °C/5 min for pre-denaturation, 95 °C/1 min; 56 °C/40 s; 72°/1 min for 35 reaction cycles, and 72 °C/5 min for elongation [16]. The sequence of primers is shown in Table 1.

2.6. Enzyme-linked immunosorbent assay (ELISA)

ELISA was to detect superoxide dismutase (SOD), malondialdehyde (MDA), and glutathione peroxidase (GSH-Px) quantitatively. Similarly, control, 1 μM AngII, 1 μM AngII +0.3 mM hirudin, 1 μM AngII +0.6 mM hirudin, and 1 μM AngII +1.2 mM hirudin were performed. ELISA plates were coated with purified SOD (no. ZC-36451, ZC-36648, ZCIBIO, China), MDA (no. ZC-36429, ZCIBIO, China), and GSH-Px antibodies (no. ZC-36648, ZCIBIO, China) in carbonate-bicarbonate buffer at 4 °C overnight. The plates were blocked with 200 μl blocking buffer BSA (1:200) (no. P0007, Beyotime. China) at 37 °C for 1 h. Then, added samples to incubated at 37 °C for 2 h and washed thrice. Horseradish peroxidase (HRP)-conjugated SOD, MDA, and GSH-Px antibodies were added to detect the specific proteins. After reaction at 37 °C for 1 h, the plates were washed thrice. Next, the wells were incubated with the substrate for approximately 10 min, and the enzyme reaction was terminated with a stop solution (no. C1058, Solarbio, China). The OD value was measured at 450 nm.

2.7. Flow cytometry analysis for ROS influence by hirudin

6-well plates were used to culture H9C2 cells. After AngII and hirudin treated cells, cells were collected and centrifuged for 5 min, 2000 rpm. H9C2 cells were fixed with 70 % alcohol. The ROS detection kit (no. S0033S, Beyotime. China) was used for flow cytometry, and the flow cytometry analyses were performed for ROS content of H9C2 cell samples including control, 1 μM AngII, 1 μM AngII +0.3 mM hirudin, 1 μM AngII +0.6 mM hirudin, and 1 μM AngII +1.2 mM hirudin.

2.8. Western blot

NLRP3 inflammasome-related proteins including NLRP3 (1:1000, no. ab263899, Abcam, USA), ASC (1:1000, no. ab283684, Abcam), pro-caspase-1(1:1000, no. ab179515, Abcam), caspase-1(1:1000, no. ab207802, Abcam), IL-1β (1:1000, no. ab254360, Abcam), IL-18 (1:1000, no. ab243091, Abcam), and mitophagy-related proteins including PINK-1 (1:1000, no. ab300623, Abcam), Parkin (1:2000, no. ab77924, Abcam), beclin-1(1:1000, no. ab302669, Abcam), LC3B (1:2000, no. ab192890, Abcam), p62 (no. ab207305, Abcam) were quantified by western blotting. β-actin as reference. Cultured H9C2 cells for 24 h with 1 μM AngII and 0, 0.3, 0.6, and 1.2 mM hirudin, respectively, PBS as a control. RIPA buffer (no. P0013K, Beyotime, China) was used for lysed samples. SDS-PAGE was used to separate lysates and proteins were transferred to polyvinylidene difluoride (PVDF) membranes. Then, the

Table 1
The primer sequence for qRT-PCR.

Gene	Forward sequence 5′-3′	Reverse sequence 5′-3′
IL-1β	ATCCTCTCCAGTCAGGCTTCCTTGTG	AGCTCTTGTCGAGATGCTGCTGTGA
IL-18	TGCCTGATATCGACCGAACAGCCAAC	ACAGATAGGGTCACAGCCAGTCCTCT
IL-6	TTCGGTACATCCTCGACGGCATCTCA	GCACAGCTCTGGCTTGTTCCTCACT
TNF-α	CAGCCAGGAGGGAGAACAGCAACT	CCGCCACGAGCAGGAATGAGAAGAG
ANP	CTCCGATAGATCTGCCCTCTTGAA	GGTACCGGAAGCTGTTGCAGCCTA
BNP	GCCAGTCTCCAGAGCAATTCA	GGGCCATTTCCT CCGACTT
β-MHC	CAGACATAGAGACCTACCTACCTC	CAGCATGTCTAGAAGCTCAGG
mtDNA	CCTATCACCCTTGCCATCAT	GAGGCTGTTGCTTGTGTGAC
β-actin	ACCGTGAAAAGATGACCCAGAT	AGCCTGGATGGCTACGTACATG
GAPDH	ACGGCAAGTTCAACGGCACAGTCA	CCACGACATACTCAGCACCAGCATCA

membranes were blocked with 5 % non-fat milk at room temperature for 1 h and incubated with primary antibodies at 4 °C. After overnight incubation, incubated with secondary antibody for 1 h. Detected the Protein expressions with high sensitivity ECL chemiluminescence detection kit (no. PK10002, Proteintech, China). Using ImageJ software (National Institutes of Health, Bethesda, MD).

2.9. Statistical analysis

Statistical analysis was conducted using GraphPad Prism 9.1.2 software. The data with means ± standard deviation (SD). For comparisons among multiple groups, one-way analysis of variance (ANOVA) or two-way ANOVA were applied. However, the difference between the two groups was analyzed by the student T-test method. Statistical significance was defined at $p < 0.05$. All the experiments were conducted in triplicate.

3. Results

3.1. Hirudin inhibits AngII-induced H9C2 cell death

CCK-8 assay was performed to quantify viability of H9C2 cells under the treatment of AngII and hirudin. As shown in Fig. 1A, 1 μM or 10 μM AngII treatment for 24 h or 36 h could significantly decrease the viability of H9C2 cells ($p < 0.001$). Next, the cell viability was not reduced by hirudin with concentrations of 0.15, 0.3, 0.6, and 1.2 mM, indicating that hirudin under these concentrations has no toxicity to H9C2 cells (Fig. 1B). Moreover, hirudin has a rescue effect on 1 μM AngII induced H9C2 cells, with a dose-dependent manner (Fig. 1C). Results screened 1 μM AngII to treat cells for 24 h, and found hirudin can relieve the inhibition of cell viability by AngII induced.

3.2. Hirudin inhibits AngII-induced H9C2 cell's hypertrophy

Phalloidine staining and ANP, BNP, and β-MHC mRNA quantifying were used to determine the hirudin effects on H9C2 cell's hypertrophy. H9C2 cells were treated with 1 μM AngII and 0.3, 0.6, 1.2 mM hirudin, and Fig. 2A shows the growth state. Fluorescence microscope was used to realize the visualization of H9C2 cell superficial area (Fig. 2B). Results showed that 1 μM AngII expanded the red area, and 0.6 and 1.2 mM hirudin significantly decreased the red area (Fig. 2C). It indicated hirudin could inhibit the H9C2 cell hypertrophy. To further demonstrate this conclusion, the expressions of myocardial hypertrophy marker genes including (Fig. 2D) ANP (Fig. 2E), BNP and (Fig. 2F) β-MHC were detected. Notably, the up-regulation of these genes by AngII induced was all inhibited by hirudin in a dose-dependent manner. It suggested that hirudin may alleviate cardiomyocyte hypertrophy and the mechanism need to further study.

3.3. Hirudin inhibited AngII-induced formation of NLRP3 inflammasome in H9C2 cells

qRT-PCR was performed to detect the expression of inflammatory cytokines, including IL-1β, IL-18, IL-6, and TNF-α (Fig. 3A). Compared with the control group, AngII caused the expression levels of IL-1β, IL-18, IL-6, and TNF-α increase about 1.53, 2.27, 1.91, and 2.70 folds, respectively. On the contrary, 1.2 mM hirudin treatment suppressed these inflammatory cytokines release. Moreover, the expressions of NLRP3 inflammasome-related proteins were analyzed using Western blot (Fig. 3B). Fig. 3C indicates that AngII significantly up-regulated these proteins including NLRP3, ASC, caspase-1, pro-caspase-1, IL-1β, and IL-18. However, these proteins expression level were decreased by 0.6 and 1.2 mM hirudin treatment. It suggesting that hirudin could inhibit the AngII-induced formation of NLRP3 inflammasome in H9C2 cells.

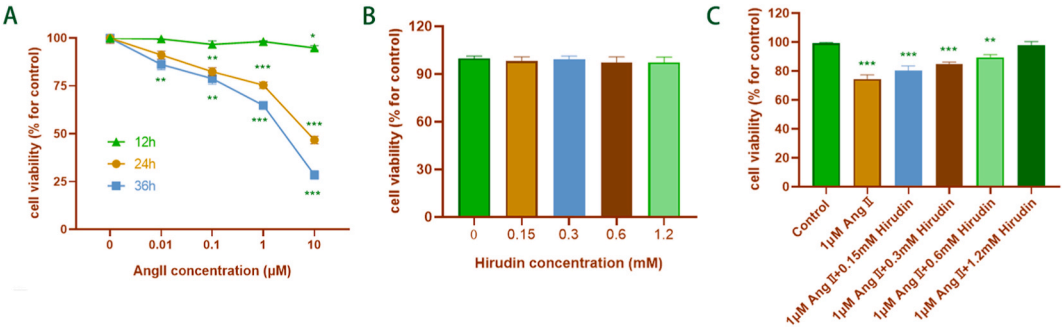

Fig. 1. Effect of hirudin on proliferation activity of H9C2 cells, H9C2 cells were treated with (0.01, 0.1, 1, and 10μM) AngII, respectively, for 12, 24, or 36h. (A) the viability of the cells was measured by CCK-8 assay. Compared to the control group, *$p<0.05$, **$p<0.01$, ***$p<0.001$. (B) H9C2 cells were treated with (0.15, 0.3, 0.6 and 1.2mM) hirudin for 24h. (C) H9C2 cells were treated with 1μM AngII and (0.15, 0.3, 0.6, or 1.2mM) hirudin for 24h. Line charts and bars represent the mean ± S.D. from three independent experiments. Compared to the control group, $^{\#\#\#}p<0.001$; Compared to the 1μM AngII group, *$p<0.05$, **$p<0.01$, ***$p<0.001$.

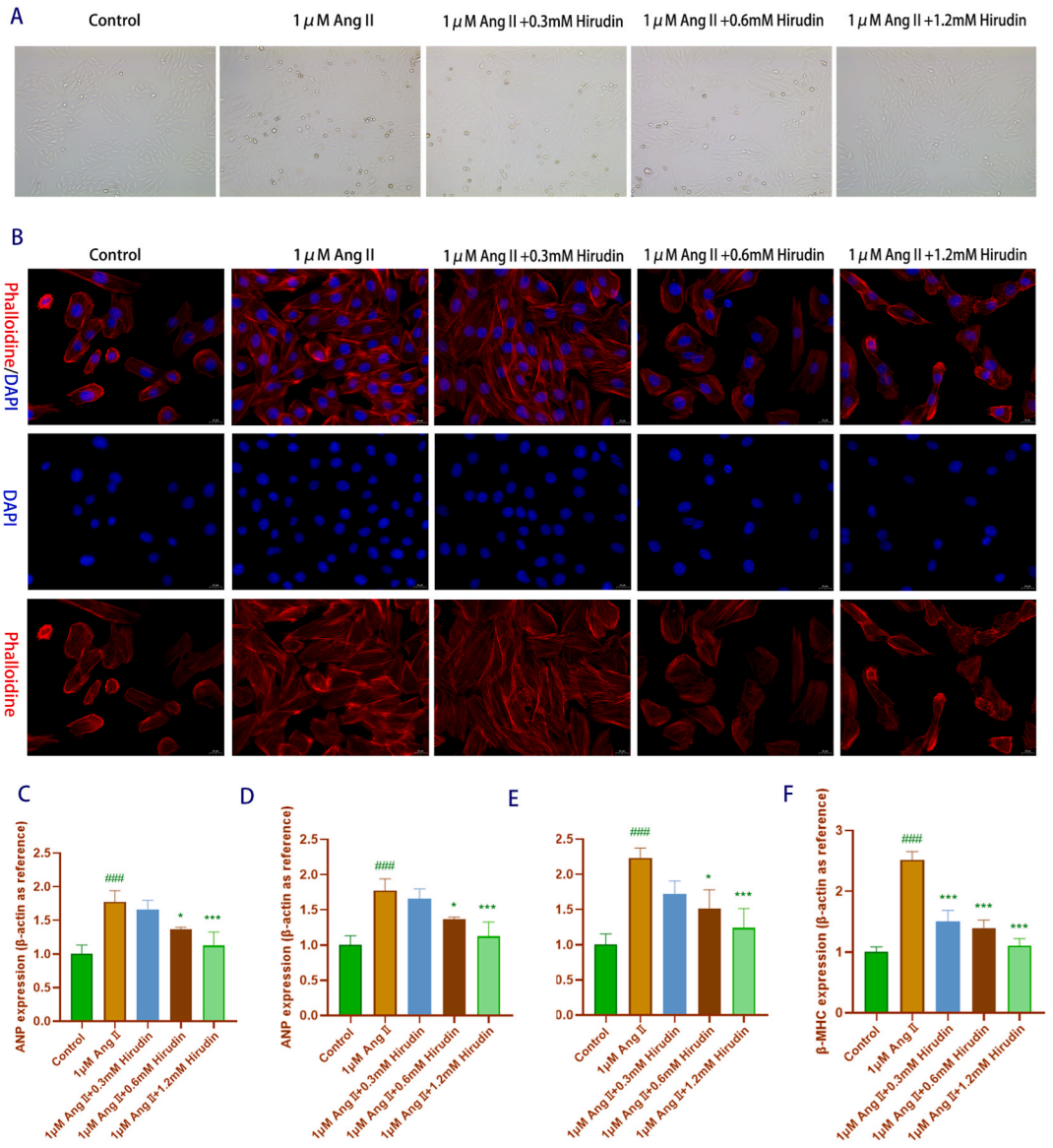

Fig. 2. Effect of hirudin on AngII-induced H9C2 cells. H9C2 cells were treated with 1μM AngII and (0.3, 0.6, or 1.2mM) hirudin, respectively, for 24h. (A) The growth state was observed by an inverted microscope. (B) phalloidine/DAPI staining, magnification: ×400. (C) Analyze of red area for phalloidine. RT-PCR was performed to detect the expressions of (D)ANP, (E) BNP, and (F) β-MHC. Bars represent the mean ± S.D. from three independent experiments. Compared to the control group, $^{###}p<0.001$; Compared to the 1μM AngII group, $^{*}p<0.05$, $^{**}p<0.01$, $^{***}p<0.001$.

3.4. Hirudin inhibited AngII-induced oxidative stress activation in H9C2 cells

To determine the hirudin effects on oxidative stress in H9C2 cells, ROS was detected by flow cytometry (Fig. 4A). The bar chart shows that AngII significantly promote ROS formation in H9C2 cells, while 0.6 and 1.2 mM hirudin shows obvious inhibition for ROS formation, and 0.3 mM hirudin has no obvious effect (Fig. 4B). Furthermore, MDA, SOD, and GSH-Px content were determined by ELISA. Among them, MDA (Fig. 4C) content was increased, and SOD (Fig. 4D) and GSH-Px (Fig. 4E) were significantly decreased by 1 μM AngII. However, hirudin (0.6, 1.2 mM) treatment reversed the status obviously. We speculated that hirudin can inhibit the AngII-induced oxidative stress and reduce cell damage.

3.5. Effects of hirudin on AngII-induced PINK-1/Parkin-mitophagy in H9C2 cells

To evaluate the effect of hirudin on mitochondrial damage, we detected the mtDNA by qRT-PCR. Fig. 5A shows that AngII could down-regulate the expression of mtDNA. However, the hirudin could increase the mtDNA expression level under AngII induce, in a

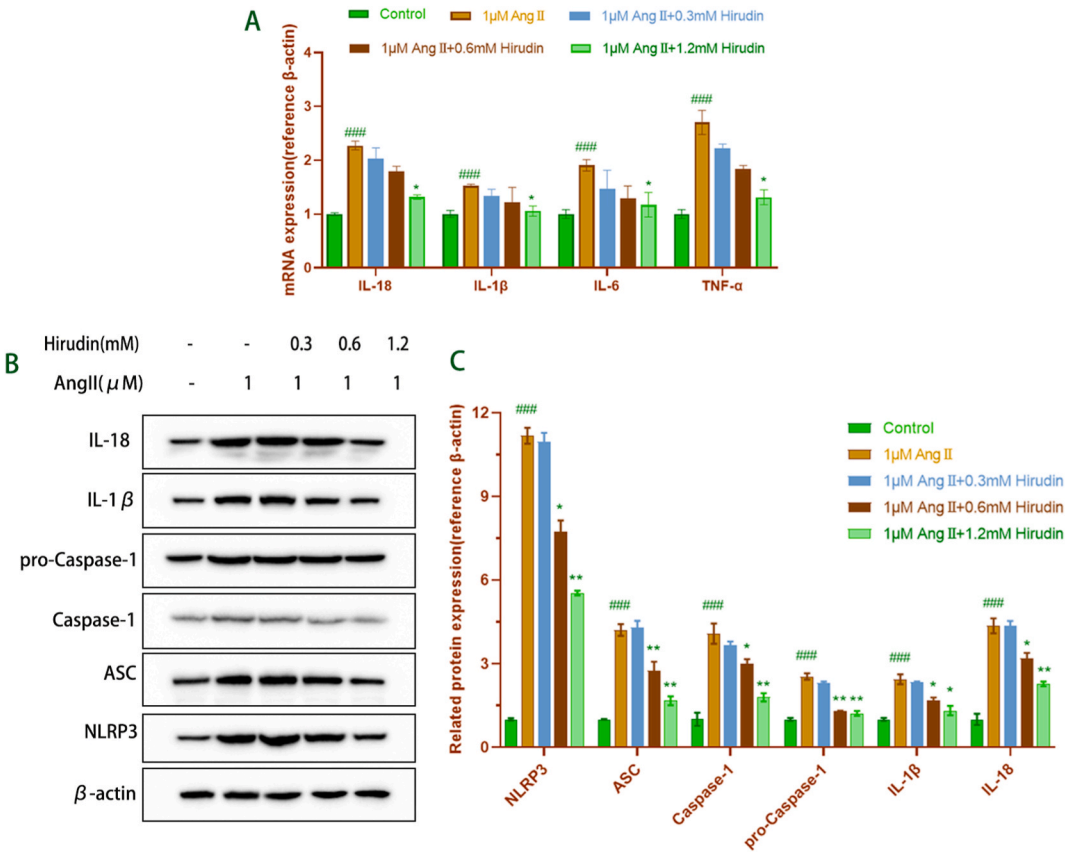

Fig. 3. Effect of hirudin on AngII-induced NLRP3 inflammasome in H9C2 cells. H9C2 cells were treated with 1μM AngII and (0.3, 0.6, or 1.2mM) hirudin, respectively, for 24h. (A) Expressions of IL-1β, IL-18, IL-6, and TNF-α were analyzed by qRT-PCR. (B) Western blot was performed for the expression of proteins including NLRP3, ASC, Caspase-1, pro-Caspase-1, IL-1β, and IL-18. (C) NLRP3, ASC, Caspase-1, pro-Caspase-1, IL-1β, and IL-18 were quantified by western blotting analysis and normalized to control. Bars represent the mean ± S.D. from three independent experiments. Compared with control group, $^{###}p<0.001$; Compared to the 1μM AngII group, $^{*}p<0.05$, $^{**}p<0.01$, $^{***}p<0.001$.

dose-dependent manner. In addition, the TEM results showed that mitophagy occurred in the four drugs treatment groups. AngII-induced group cells had less autophagic vacuole than the hirudin treatment groups. Especially, with the hirudin dose increasing, the quantity of autophagic vacuole increased compared to the control group (Fig. 5B). These results demonstrated that hirudin could suppress mitochondrial damage. Therefore, WB was performed to evaluate the expression of mitophagy-related proteins, including PINK-1, Parkin, beclin-1, LC3-I, LC3-II, and p62 (Fig. 5C). AngII stimulation could increase the ratio of LC3-II/LC3-I (Fig. 5E) and up-regulated the expression of beclin-1 and p62 (Fig. 5D). Furthermore, AngII did not affect PINK-1 and Parkin (Fig. 5D). However, in hirudin treatment groups, with the hirudin dose increasing, the expression of related proteins and LC3-II/LC3-I ratio were increasing (Fig. 5D/E). It demonstrated that hirudin may activate mitophagy by activating PINK-1/Parkin pathway to inhibiting myocardial hypertrophy.

4. Discussion

Angiotensin II (AngII) is a fundamental mediator of cardiac remodeling, leading to heart fibrosis and hypertrophy when excessively secreted [17]. It plays a pivotal role in the development of cardiac disease. Therefore, inhibiting the effects of AngII is an effective approach for treating cardiac hypertrophy. Hirudin, the primary active component found in leeches, is commonly utilized as a thrombin-specific inhibitor.

In recent years, hirudin has been shown to possess various other biological activities. For instance, *Xie, Y* et al. reported that hirudin reduces interstitial fibrosis by inhibiting inflammation [18]. Liu, W. et al. demonstrated that hirudin exhibits scavenging activity for ROS, and can inhibit the activation of the NF-kB pathway [19]. Previously, hirudin's inhibitory activity on cardiac hypertrophy [20]. However, its' molecular mechanism remains unclear at present. In this study, we have discovered that hirudin can significantly reduce the superficial area of AngII-induced H9C2 cells and mitigate the toxicity of AngII for these cells. Notably, at a concentration of 1.2 mM, Hirudin displayed no toxicity to H9C2 cells. Specifically, well-established cardiac hypertrophy biomarkers including ANP, BNP, and β-MHC were investigated [21]. The results indicated that hirudin is capable of inhibiting the expressions of ANP, BNP, and β-MHC,

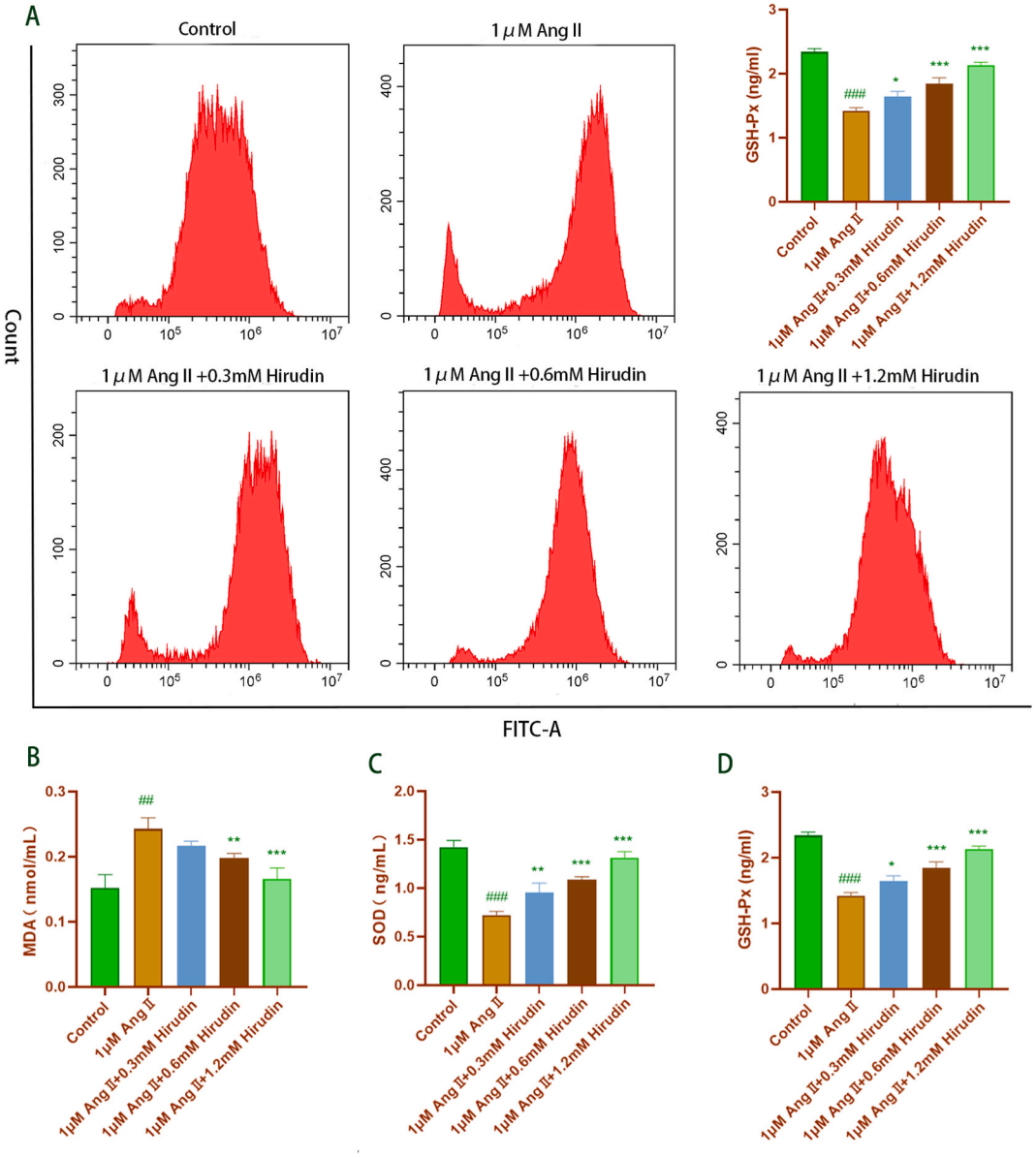

Fig. 4. Effect of hirudin on AngII-induced oxidative stress activation in H9C2 cells. H9C2 cells were treated with 1μM AngII and (0.3, 0.6, or 1.2mM) hirudin, respectively, for 24h. (A) Flow cytometry was used to detect Ros. (B) Ros was quantified by the mean fluorescence intensity of FITC. Elisa was performed to detect the expression of MDA(C), SOD(D), and GSH-Px(E). Bars represent the mean ± S.D. from three independent experiments. Compared with control group, $^{\#\#}p<0.01$, $^{\#\#\#}p<0.001$; Compared to the 1μM AngII group, $^{*}p<0.05$, $^{**}p<0.01$, $^{***}p<0.001$.

thereby exerting an inhibitory effect on cardiac hypertrophy. These findings lay the groundwork for potential clinical applications of hirudin in the treatment of cardiac hypertrophy.

Increasing evidence indicated that NLRP3 inflammasome plays a key role in the initiation and progression of cardiac hypertrophy [22]. Research reports have suggested that inhibiting the activation of NLRP3 inflammasome can hinder the pathological cardiac remodeling [22]. Considering that NLRP3 inflammasome was composed of NLRP3, ASC, and Pro-caspase-1 [23]. Upon activation of the NLRP3 inflammasome, there is an increase in the expression of NLRP3, ASC, Pro-caspase-1, and caspase-1. Furthermore, NLRP3 inflammasome activation leads to the secretion of cytokines such as IL-1β and IL-18 [23], both of which participate in cardiac hypertrophy. It is reported that IL-1β play a pivotal role in promoting senility in the cardiac fibroblast [24], while pressure overload-induced overexpression of IL-18 contributes to the development of cardiac hypertrophy [25]. Additionally, researchers have reported that knockout TNF-α can inhibit cardiac hypertrophy, whereas IL-6 drives the progression of pathologic hypertrophy and fibrosis [26,27]. In this study, our experiments demonstrated that hirudin down-regulated NLRP3 inflammasome-related proteins in AngII-induced H9C2 cells in a dose-dependent manner. These proteins include NLRP3, ASC, caspase-1, pro-caspase-1, IL-1β, and IL-18.

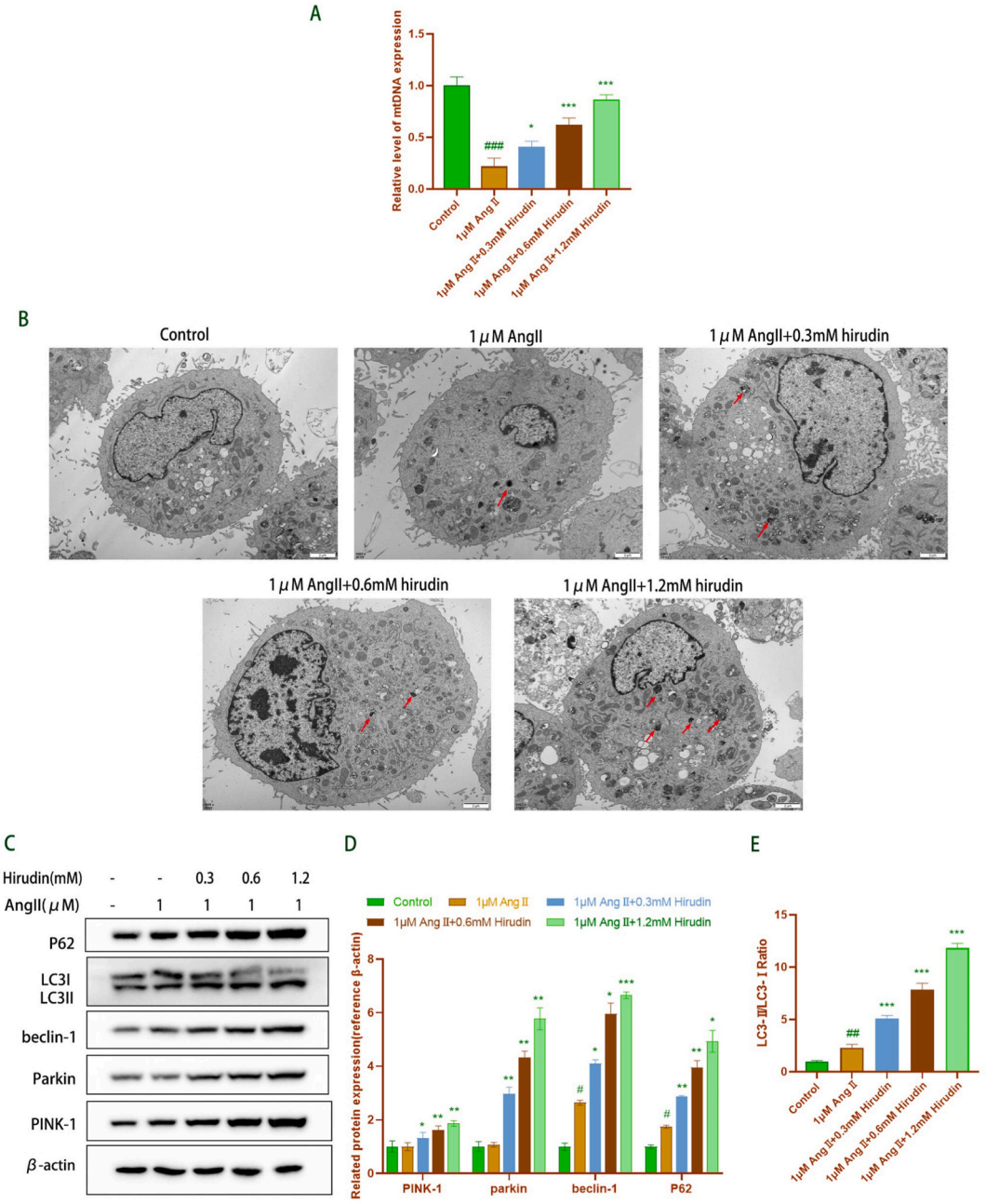

Fig. 5. Effect of hirudin on AngII induced PINK-1/Parkin-mitochondrial autophagy in H9C2 cells. H9C2 cells were treated with 1μM AngII and (0.3, 0.6, or 1.2mM) hirudin, respectively, for 24h. (A) The expression of mtDNA was analyzed by qRT-PCR. (B) Transmission electron microscopy (TEM) was used to observe the formation of autophagosomes (red arrow). (C) Western blot was performed for the expression of proteins including PINK-1, Parkin, beclin-1, LC3-I, LC3-II, and P62. (D) PINK-1, Parkin, beclin-1, LC3-I, LC3-II, and P62 were quantified by western blotting analysis and normalized to control. (E) LC3-II/ LC3-I Ratio. Compared with control group, $^{\#}p<0.05$, $^{\#\#}p<0.01$, $^{\#\#\#}p<0.001$; Compared to the 1μM AngII group, $^{*}p<0.05$, $^{**}p<0.01$, $^{***}p<0.001$.

Furthermore, NLRP3 inflammasome-related cytokines containing IL-6 and TNF-α were down-regulated by hirudin too. Collectively, these findings indicate that hirudin treatment effectively blocked the activation of NLRP3 inflammasome and downregulated the pro proinflammatory cytokines including IL-1β, IL-18, IL-6, and TNF-α expression caused by AngII. This provides a promising foundation for cardiac hypertrophy treatment.

Prior research has highlighted the significant role of hirudin in NLRP3 inflammasome activation [28]. As reported, mitochondria are the major sites for ROS generation. When the balance between ROS clearance and production is disrupt, accumulated ROS can lead

to mitochondrial damage [29]. Subsequently, damaged mitochondrial releases mtDNA, which then fuses with NLRP3, resulting in the activation of the NLRP3 inflammasome [30]. Therefore, there exists a reciprocal interaction between ROS, mitophagy, and NLRP3 inflammasome activation. Our experiments confirmed that hirudin down-regulated the expression of ROS, decreased the MDA, and increased SOD, and GSH-Px. These enzymes contain SOD and GSH-Px, with the function of elimination of ROS. Moreover, TEM results showed that hirudin significantly increased mitophagy. In summary, hirudin treatment effectively mitigated the ROS production induced by AngII, and suppressed the activation of the NLRP3 inflammasome.

Furthermore, mitophagy-related proteins, including PTEN-induced kinase 1(PINK-1), Parkin, beclin-1, LC3-I, LC3-II, and p62, were quantified. Notably, the expressions of PINK-1, Parkin, beclin-1, and p62 and the ratio of LC3-II/LC3-I were up-regulated by hirudin all, in a dose-dependent manner. As reported, with the mitophagy increasing, expressions of these proteins increased [31]. PINK-1 accumulates on the outer mitochondrial membrane and activates the PARKIN, which in turn recruits the LC3-binding protein p62 into mitochondria [32]. Importantly, when p62 is absent, the clearance of damaged mitochondria is entirely blocked [33]. Our experiments demonstrated that mitophagy was enhanced by hirudin in AngII-induced H9C2 cells.

In summary, hirudin demonstrates a multifaceted impact on the processes underlying AngII-induced cardiac hypertrophy. By reducing ROS levels and down-regulating mtDNA, hirudin effectively inhibits the activation of the NLRP3 inflammasome, thereby impeding the progression of mitophagy. This intricate interplay among ROS, mtDNA, NLRP3 inflammasome, and mitophagy constitutes a feedback loop contributing to cardiac hypertrophy. Blocking any of these stages disrupts the cascade, ultimately alleviating cardiac hypertrophy. It is important to acknowledge that our study's limitation lies in the absence of animal experimentation to validate the effects of hirudin, although we intend to address this in the near future. Our investigation delved into the underlying mechanism through which hirudin counteracts cardiac hypertrophy in an in vitro context, focusing on the modulation of NLRP3 inflammasome activation. This study lays the groundwork for potential clinical applications of hirudin in the treatment of cardiac hypertrophy. As we move forward, subsequent animal studies will provide further insights into the therapeutic potential of hirudin.

Funding

This work was supported by the National Natural Science Foundation of China (82074378), the National TCM Inheritance and Innovation Team (ZYYCXTD-C-202207), Sichuan Science and Technology Program (2022YFS0618) and Luzhou Science and Technology Bureau Project (2022JYJ104, 2023JYJ029), Southwest Medical University Project (22ZDYF3795). The funder had no role in the study design, data analysis, or decision to publish.

Data availability statement

The data sets used and analyzed during the current study are available from the corresponding author upon reasonable request.

CRediT authorship contribution statement

Gang Luo: Writing - review & editing, Writing - original draft, Conceptualization. **Li Chen:** Writing - original draft, Investigation, Formal analysis, Data curation. **Mingtai Chen:** Writing - original draft, Investigation, Formal analysis, Data curation. **Linshen Mao:** Writing - original draft, Investigation, Formal analysis, Data curation. **Qihu Zeng:** Validation, Funding acquisition. **Yuan Zou:** Formal analysis, Data curation. **Jinyi Xue:** Formal analysis, Data curation. **Ping Liu:** Writing - review & editing, Writing - original draft, Project administration. **Qibiao Wu:** Writing - review & editing, Writing - original draft, Project administration. **Sijin Yang:** Writing - review & editing, Writing - original draft, Project administration. **Mengnan Liu:** Writing - review & editing, Writing - original draft, Project administration, Conceptualization.

Declaration of competing interest

The authors declare the following financial interests/personal relationships which may be considered as potential competing interests:Sijin Yang reports administrative support was provided by National Natural Science Foundation of China. Ping Liu reports administrative support was provided by Sichuan Province Science and Technology Support Program. Mengnan Liu reports financial support and administrative support were provided by Luzhou Science and Technology Bureau Project. Mengnan Liu reports administrative support was provided by Southwest Medical University Project. If there are other authors, they declare that they have no known competing financial interests or personal relationships that could have appeared to influence the work reported in this paper.

Acknowledgements

Thank you to Professor Sijin Yang, Professor Qibiao Wu, and Dr. Li Chen for their strict technical guidance on this study.

Appendix A. Supplementary data

Supplementary data to this article can be found online at https://doi.org/10.1016/j.heliyon.2023.e23077.

References

[1] S. Gallo, A. Vitacolonna, A. Bonzano, et al., ERK: a key player in the pathophysiology of cardiac hypertrophy, Int. J. Mol. Sci. 20 (9) (2019), https://doi.org/10.3390/ijms20092164.

[2] D.S. Souza, T.O. Barreto, J.E.R. Menezes-Filho, et al., Myocardial hypertrophy is prevented by farnesol through oxidative stress and ERK1/2 signaling pathways, Eur. J. Pharmacol. 887 (2020), 173583, https://doi.org/10.1016/j.ejphar.2020.173583.

[3] B. Ren, J. Feng, N. Yang, et al., Ginsenoside Rg3 attenuates angiotensin II-induced myocardial hypertrophy through repressing NLRP3 inflammasome and oxidative stress via modulating SIRT1/NF-kappaB pathway, Int. Immunopharm. 98 (2021), 107841, https://doi.org/10.1016/j.intimp.2021.107841.

[4] L. Song, L. Pei, S. Yao, et al., NLRP3 inflammasome in neurological diseases, from functions to therapies, Front. Cell. Neurosci. 11 (2017) 63, https://doi.org/10.3389/fncel.2017.00063.

[5] K. Miteva, K. Pappritz, M. Sosnowski, et al., Mesenchymal stromal cells inhibit NLRP3 inflammasome activation in a model of Coxsackievirus B3-induced inflammatory cardiomyopathy, Sci. Rep. 8 (1) (2018) 2820, https://doi.org/10.1038/s41598-018-20686-6.

[6] M. Lamkanfi, Emerging inflammasome effector mechanisms, Nat. Rev. Immunol. 11 (3) (2011) 213–220, https://doi.org/10.1038/nri2936.

[7] M.E. Heid, P.A. Keyel, C. Kamga, et al., Mitochondrial reactive oxygen species induces NLRP3-dependent lysosomal damage and inflammasome activation, J. Immunol. 191 (10) (2013) 5230–5238, https://doi.org/10.4049/jimmunol.1301490.

[8] V. Deretic, T. Kimura, G. Timmins, et al., Immunologic manifestations of autophagy, J. Clin. Invest. 125 (1) (2015) 75–84, https://doi.org/10.1172/JCI73945.

[9] E.S. Kang, J.S. Hwang, W.J. Lee, et al., Ligand-activated PPARdelta inhibits angiotensin II-stimulated hypertrophy of vascular smooth muscle cells by targeting ROS, PLoS One 14 (1) (2019), e0210482, https://doi.org/10.1371/journal.pone.0210482.

[10] X. Hou, Z. Hu, H. Xu, et al., Advanced glycation endproducts trigger autophagy in cadiomyocyte via RAGE/PI3K/AKT/mTOR pathway, Cardiovasc. Diabetol. 13 (2014) 78, https://doi.org/10.1186/1475-2840-13-78.

[11] C. Junren, X. Xiaofang, Z. Huiqiong, et al., Pharmacological activities and mechanisms of hirudin and its derivatives - a review, Front. Pharmacol. 12 (2021), 660757, https://doi.org/10.3389/fphar.2021.660757.

[12] W.L. Cao, J. Li, [Antithrombotic effects of recombinant hirudin in mice and its mechanism], Zhongguo Ying Yong Sheng Li Xue Za Zhi 34 (4) (2018) 371–374, https://doi.org/10.12047/j.cjap.5664.2018.085.

[13] M. Liu, G. Luo, L. Dong, et al., Network pharmacology and in vitro experimental verification reveal the mechanism of the hirudin in suppressing myocardial hypertrophy, Front. Pharmacol. 13 (2022), 914518, https://doi.org/10.3389/fphar.2022.914518.

[14] V. Kundumani-Sridharan, N.K. Singh, S. Kumar, et al., Nuclear factor of activated T cells c1 mediates p21-activated kinase 1 activation in the modulation of chemokine-induced human aortic smooth muscle cell F-actin stress fiber formation, migration, and proliferation and injury-induced vascular wall remodeling, J. Biol. Chem. 288 (30) (2013) 22150–22162, https://doi.org/10.1074/jbc.M113.454082.

[15] J. Wall, S. Naganathar, B. Praditsuktavorn, et al., Modeling cardiac dysfunction following traumatic hemorrhage injury: impact on myocardial integrity, Front. Immunol. 10 (2019) 2774, https://doi.org/10.3389/fimmu.2019.02774.

[16] E. Girsang, C.N. Ginting, I.N.E. Lister, et al., Anti-inflammatory and antiaging properties of chlorogenic acid on UV-induced fibroblast cell, PeerJ 9 (2021), e11419, https://doi.org/10.7717/peerj.11419.

[17] L. Schirone, M. Forte, S. Palmerio, et al., A review of the molecular mechanisms underlying the development and progression of cardiac remodeling, Oxid. Med. Cell. Longev. 2017 (2017), 3920195, https://doi.org/10.1155/2017/3920195.

[18] Y. Xie, F. Lan, J. Zhao, et al., Hirudin improves renal interstitial fibrosis by reducing renal tubule injury and inflammation in unilateral ureteral obstruction (UUO) mice, Int. Immunopharm. 81 (2020), 106249, https://doi.org/10.1016/j.intimp.2020.106249.

[19] W. Liu, X.C. Liang, Y. Shi, Effects of hirudin on high glucose-induced oxidative stress and inflammatory pathway in rat dorsal root ganglion neurons, Chin. J. Integr. Med. 26 (3) (2020) 197–204, https://doi.org/10.1007/s11655-019-2712-8.

[20] S. Wang, C. Wu, Y. Li, et al., Analysis of the anti-tumour effect of xuefu zhuyu decoction based on network pharmacology and experimental verification in Drosophila, Front. Pharmacol. 13 (2022), 922457, https://doi.org/10.3389/fphar.2022.922457.

[21] H.Q. Sun, D. Yan, Q.N. Wang, et al., 1,25-Dihydroxyvitamin D3 attenuates disease severity and induces synoviocyte apoptosis in a concentration-dependent manner in rats with adjuvant-induced arthritis by inactivating the NF-kappaB signaling pathway, J. Bone Miner. Metabol. 37 (3) (2019) 430–440, https://doi.org/10.1007/s00774-018-0944-x.

[22] M. Zhao, J. Zhang, Y. Xu, et al., Selective inhibition of NLRP3 inflammasome reverses pressure overload-induced pathological cardiac remodeling by attenuating hypertrophy, fibrosis, and inflammation, Int. Immunopharm. 99 (2021), 108046, https://doi.org/10.1016/j.intimp.2021.108046.

[23] S.K. Vanaja, V.A. Rathinam, K.A. Fitzgerald, Mechanisms of inflammasome activation: recent advances and novel insights, Trends Cell Biol. 25 (5) (2015) 308–315, https://doi.org/10.1016/j.tcb.2014.12.009.

[24] J.A. Espitia-Corredor, L. Shamoon, F. Olivares-Silva, et al., Resolvin E1 attenuates doxorubicin-induced cardiac fibroblast senescence: a key role for IL-1beta, Biochim. Biophys. Acta, Mol. Basis Dis. 1868 (11) (2022), 166525, https://doi.org/10.1016/j.bbadis.2022.166525.

[25] N. Matsushita, N. Ishida, M. Ibi, et al., Chronic pressure overload induces cardiac hypertrophy and fibrosis via increases in SGLT1 and IL-18 gene expression in mice, Int. Heart J. 59 (5) (2018) 1123–1133, https://doi.org/10.1536/ihj.17-565.

[26] C.J. Chiang, Y.P. Chao, A. Ali, et al., Probiotic Escherichia coli Nissle inhibits IL-6 and MAPK-mediated cardiac hypertrophy during STZ-induced diabetes in rats, Benef. Microbes 12 (3) (2021) 283–293, https://doi.org/10.3920/BM2020.0094.

[27] D. Chen, Z. Li, P. Bao, et al., Nrf2 deficiency aggravates Angiotensin II-induced cardiac injury by increasing hypertrophy and enhancing IL-6/STAT3-dependent inflammation, Biochim. Biophys. Acta, Mol. Basis Dis. 1865 (6) (2019) 1253–1264, https://doi.org/10.1016/j.bbadis.2019.01.020.

[28] T. Luo, X. Jia, W.D. Feng, et al., Bergapten inhibits NLRP3 inflammasome activation and pyroptosis via promoting mitophagy, Acta Pharmacol. Sin. (2023), https://doi.org/10.1038/s41401-023-01094-7.

[29] Y. Wang, L. He, D. Du, et al., A metabolomics-based study on NMDAR-mediated mitochondrial damage through calcium overload and ROS accumulation in myocardial infarction, Front Biosci (Landmark Ed) 28 (7) (2023) 140, https://doi.org/10.31083/j.fbl2807140.

[30] H. Ahn, J. Kim, S.G. Kang, et al., Mercury and arsenic attenuate canonical and non-canonical NLRP3 inflammasome activation, Sci. Rep. 8 (1) (2018), 13659, https://doi.org/10.1038/s41598-018-31717-7.

[31] J. Qi, Q. Xue, L. Kuang, et al., Berberine alleviates cisplatin-induced acute kidney injury by regulating mitophagy via PINK 1/Parkin pathway, Transl. Androl. Urol. 9 (4) (2020) 1712–1724, https://doi.org/10.21037/tau-20-1129.

[32] L. Li, T. Huang, J. Yang, et al., PINK1/Parkin pathway-mediated mitophagy by AS-IV to explore the molecular mechanism of muscle cell damage, Biomed. Pharmacother. 161 (2023), 114533, https://doi.org/10.1016/j.biopha.2023.114533.

[33] R. Lan, J.T. Wu, T. Wu, et al., Mitophagy is activated in brain damage induced by cerebral ischemia and reperfusion via the PINK1/Parkin/p62 signalling pathway, Brain Res. Bull. 142 (2018) 63–77, https://doi.org/10.1016/j.brainresbull.2018.06.018.